



# DESIGN A 2x2 COMPACT MODE SWITCHING USING MULTIMODE INTERFERENCE BASED ON SILICON MATERIAL

Ho Duc Tam Linh\*, Nguyen Phuoc Nhat, Vuong Quang Phuoc, Dao Duy Tu

Department of Electronics and Telecommunications, University of Sciences, Hue University

**Abstract.** We propose a new design of a 2x2 optical chip for switching optical modes based on silicon material. Input lights at fundamental mode of transverse electric (TE) polarization can be selected at the output by appropriately controlling a 180-degree butterfly-shaped phase shifter. The proposed device consists of two multimode interference waveguides MMI and a phase shifter packed in a compact size of  $4.2\mu\text{m} \times 0.22\mu\text{m} \times 110.4\mu\text{m}$ . We use 3D-BPM numerical simulation method to evaluate optical conversion efficiency of device. The result shows that insertion loss is always less than 1.5dB and crosstalk is always below -30dB in a wavelength range from  $1.5\mu\text{m}$  to  $1.6\mu\text{m}$ . Moreover, we continue to evaluate the proposed device on the system with signal's bitrate of 35Gbps, the bit error rate is always less than  $10^{-10}$  in the whole bandwidth of 100nm.

**Keywords:** multimode interference, phase shifter, 3D-BPM, silicon

## 1 Introduction

The 4<sup>th</sup> Industrial Revolution [1] is going on with a rapid increase in broadband data services, so extending transmission bandwidth is an urgent issue in the communication systems. To increase the data capacity, some different signal multiplexing technologies have been used in optical fiber communications such as wavelength division multiplexing (WDM) [2-6], time division multiplexing (TDM) [7], polarization division multiplexing (PDM) [8]... Recently, a new technology, mode division multiplexing (MDM) technology [9-14], which is expected to be a promising technology to significantly increase the capacity to the number of modes. In MDM technique, data channels are independently carried on orthogonal eigenmodes of the same wavelength to increase capacity of optical communications. To meet the future broadband telecom and on-chip communication application [15-16], mode switch featuring with small-footprint, wideband, low loss, small-crosstalk operations and simple fabrication are particularly desirable to realize compact photonic integrated circuits that could work simultaneously for MDM and WDM signals.

---

\* Corresponding: [hdtlinh@hueuni.edu.vn](mailto:hdtlinh@hueuni.edu.vn)

A recently article has showed a mode division multiplexing switching device on optical chip that has been demonstrated experimentally using a Y junction structure and a MMI coupler [17]. The switching between the ports is achieved by a lateral PN junction. The device can perform switches for 2 modes TE<sub>0</sub> and TE<sub>1</sub>, simulated insertion loss is less than 0.3dB for both TE<sub>0</sub> and TE<sub>1</sub> inputs over the wavelength range from 1530nm to 1570nm but a disadvantage of this device is quite large in size, approximately 400μm in length. Next, another research used 2 MMI couplers and a thermo-optic phase shifter to design a switching device [18], but the device's insertion loss is quite high up to 1dB at the central wavelength. However, the general characteristics of those devices has not evaluated performance on the system.

In this paper, we study to combine the advantages of these two MMI structures to create a 2x2 mode switching device using silicon on insulator with switching the modes TE<sub>0</sub> between two inputs and two outputs. The high optical conversion efficiency over 97% and compact size of 4.2μm × 0.22μm × 110.4μm are advantages of the proposed device. In addition, we evaluate the fabrication tolerance of the device, the results demonstrate that the device can work well with a large manufacturing errors. Moreover, we also evaluate the effectiveness of devices on complex communication systems, the simulation results show that the device can operate effectively with performance more than 70% in a wide bandwidth up to 100nm. Furthermore, the proposed device can work with an extremely high bit rate of up to 35Gbps while bit error rate is always remained smaller than 10<sup>-10</sup>.

## 2 Device structure and design principle.

### 2.1 MMI theory

The self-imaging phenomenon is the basic properties in waveguides as stated by Soldano [19]. The beat length  $L_\pi$  is an important parameter to determine the appropriate length in order to create the desired periodic images in the waveguide as shown in Figure 1, this beat length is defined by two lowest-order modes in the MMI and it is given by formula

$$L_\pi = \frac{4n_{\text{eff}}W_{\text{eff}}^2}{3\lambda} \quad (1)$$

$$W_{\text{eff}} = W_{\text{MMI}} + \frac{\lambda_0}{\pi} \left( \frac{n_c}{n_r} \right)^{2\sigma} (n_r^2 - n_c^2)^{-(1/2)} \quad (2)$$

For  $\sigma = 0$  (TE mode),  $\sigma = 1$  (TM mode) and where  $W_{\text{eff}}$ ,  $\lambda$ ,  $n_{\text{eff}}$ ,  $n_r$  and  $n_c$  are the effective width of MMI, wavelength, effective refractive index, core (effective) refractive index and cladding (effective) refractive index, respectively.

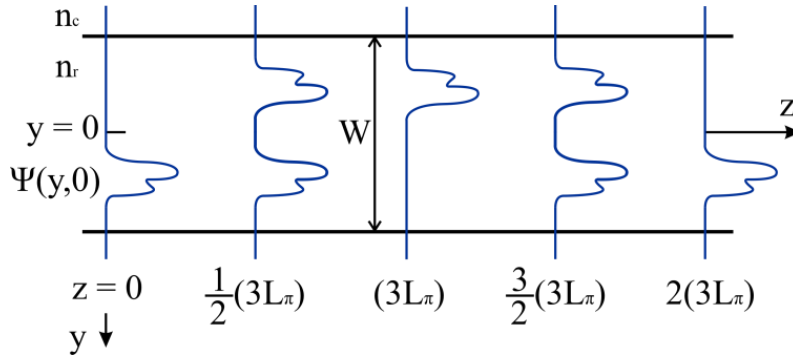


Fig. 1. The self-imaging theory in 2x2 MMI coupler

The self-imaging in waveguide is created by one of two interference mechanisms: general interference and restricted interference mechanisms.

For general interference mechanism is shown by formula

$$L_{MMI} = \frac{p}{N}(3L_{\pi}) \tag{3}$$

And restricted interference mechanism

$$L_{MMI} = \frac{p}{N}(L_{\pi}) \tag{4}$$

Where N is the number of input and output ports of the MMI, p denotes the periodic properties of image along the MMI. We usually choose p = 1 to shorten the size of the device as much as possible. Comparing between two interference mechanisms above, notice that the length of devices using the restricted interference mechanism is three times shorter than that using the general interference mechanism.

### 2.2 Phase shifter

The phase shifter plays an important role in this article with the aim of controlling the signal path in waveguides. We choose the fixed length  $L_{ps}$  of  $16.8\mu\text{m}$  as described in Figure 3. By varying the center width of the phase shifter as shown in Figure 2, the phase difference between input and output port also will vary. From the simulation result is indicated in Figure 2, if the center width of the phase shifter  $W_{ps} = 0.35\mu\text{m}$  then the phase difference at output port is 180 degrees. This phase difference will be 90 degrees when  $W_{ps} = 0.38\mu\text{m}$ .

### 2.3 Structure design

Structure of the mode switch is shown in Figure 3. The proposed switch consists of two 2x2 MMI couplers that are linked together by access waveguides. The width of these access

waveguides is selected  $W_{in} = 0.3\mu\text{m}$  to support one  $TE_0$  fundamental modes. They are posited in  $\pm W_{MMI}/6$  position compared to center position of the MMI region. In this design, we choose width of the MMI region as  $W_{MMI} = 4.8\mu\text{m}$ , and its length is chosen as  $L_{MMI} = L_{\pi}/2 = 22.8\mu\text{m}$ . To improve transmission efficiency between the access waveguides and MMI device, a taper will be used with the length  $L_{tp}$  and width  $W_{tp}$  of  $7\mu\text{m}$  and  $0.85\mu\text{m}$ , respectively. The height of device is  $H = 0.22\mu\text{m}$ .

The device is based on SOI (Silicon on Insulator) material platform with channel structure. The core layer is made of silicon with refractive index  $n_r = 3.47$  while cladding layer is made of silica with refractive index  $n_c = 1.44$ .

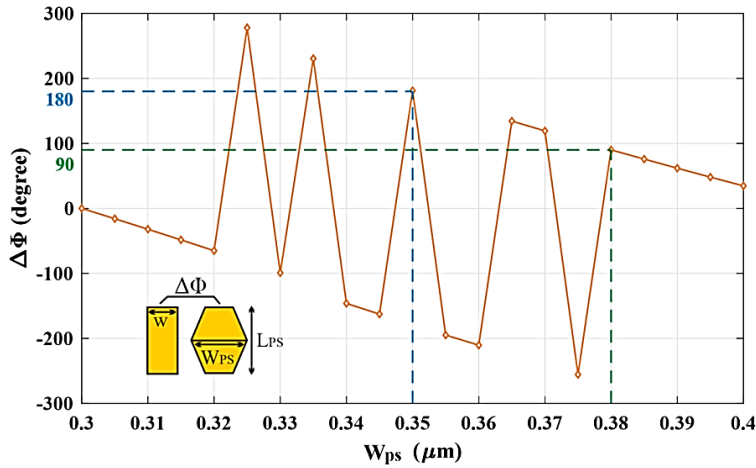


Fig. 2. Surveying the phase difference at output of the phase shifter by varying the center width

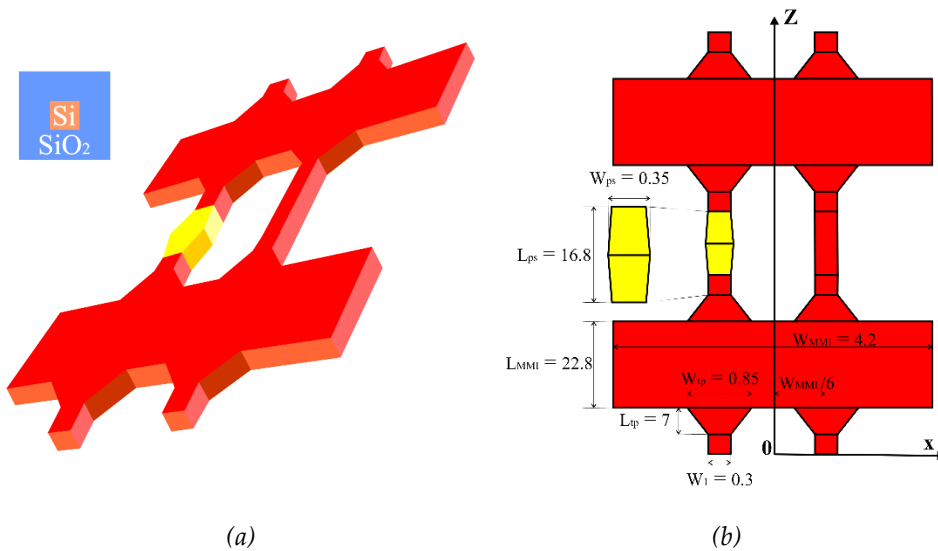
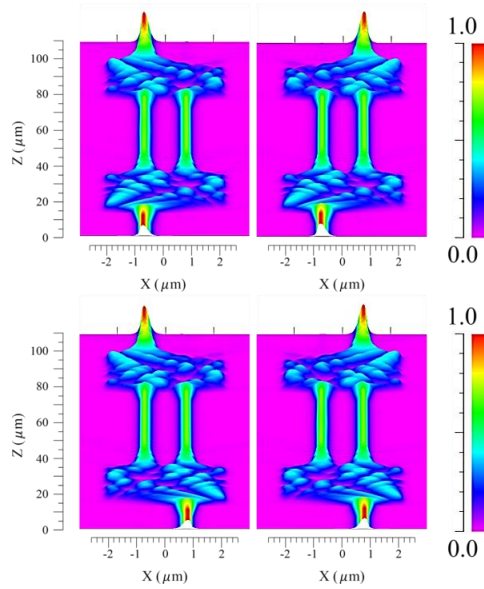


Fig. 3. The general schematic and parameters of the proposed switch, (a) 3D, (b) 2D



**Fig. 4.** Electric field patterns of proposed switching device

From these electric field patterns (Figure 4), we can observe a very small amount of light radiated out of guided-wave regions, which can be shown that the optical conversion efficiency is also very high. Figure 4 shows the field distribution of the optical mode switch at wavelength of  $1.55\mu\text{m}$  when fundamental mode is launched to the device. To better understand this issue, we will explain the principle of operation as follows:

1. When there is no phase shifter: if a signal is launched at input  $I_1$ , the output  $O_2$  will receive the signal. Otherwise, the output  $O_1$  will obtain the signal if a signal is transmitted at input  $I_2$ .
2. When the phase shifter is added to the device: if a signal is launched at input  $I_1$ , the output  $O_1$  will receive the signal. If a signal is transmitted at input  $I_2$ , the output  $O_2$  will surely obtain the signal from input  $I_2$ .

Besides, we also evaluate the optical performances of the proposed device by using 3D-BPM numerical simulation method. The important parameters taken into account are insertion loss (I.L) and crosstalk (CT) which are defined by

$$\text{IL (dB)} = 10 \log_{10} \frac{P_{\text{out-desirable}}}{P_{\text{in}}} \quad (5)$$

$$\text{CT (dB)} = 10 \log_{10} \frac{P_{\text{out-unwanted}}}{P_{\text{out-desirable}}} \quad (6)$$

Where  $P_{in}$  is the input power of the device,  $P_{out-desirable}$  is the received power at the desired output and  $P_{out-unwanted}$  is the leakage power at the another output.

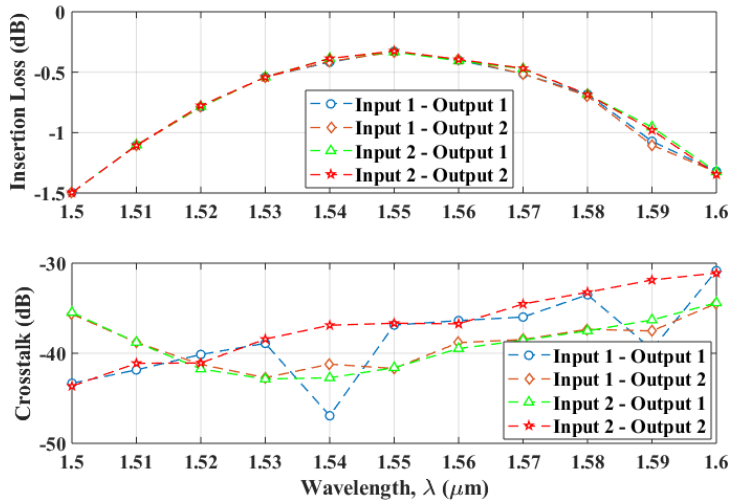


**Fig. 5.** Insertion loss and crosstalk of the proposed optical mode switching as a function of the wavelength

Figure 5 shows the graph of insertion loss and crosstalk. At the central wavelength  $\lambda = 1.55\mu\text{m}$ , insertion loss and crosstalk are less than 0.5dB and -35dB, respectively. Furthermore, if we expand the wide bandwidth range to 100nm, the insertion loss is also less than 1.5dB and crosstalk is always less than -30dB.

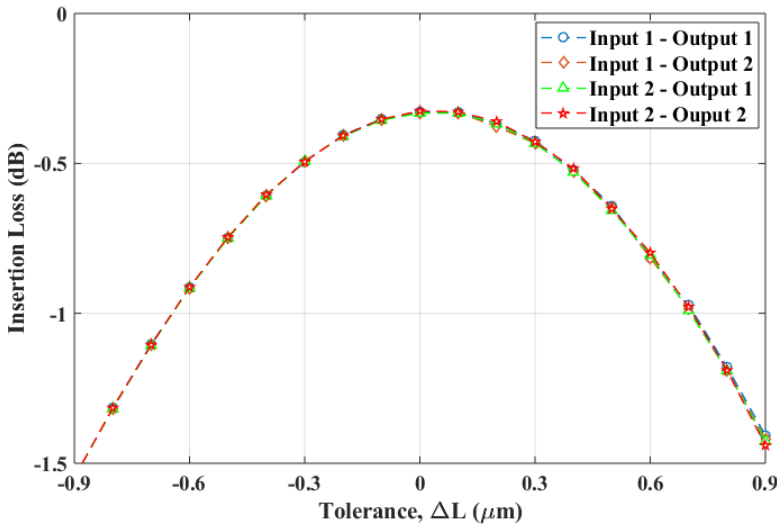


**Fig. 6.** Tolerance of the proposed switching device on variation of the MMI length

Next, we examine the tolerance of the device which is very important to etch and manufacture it in practice. We evaluate two important parameters of the devices, the length and

width of MMI region corresponding to its tolerance is  $\Delta L_{\text{MMI}}$  and  $\Delta W_{\text{MMI}}$ . From figures 6 and 7, if the length of MMI region of  $L_{\text{MMI}} = 23.2 \pm 0.9 \mu\text{m}$  and the width of MMI region of  $W_{\text{MMI}} = 4.8 \pm 0.05 \mu\text{m}$ , insertion loss always less than 1.5dB and 1dB, respectively. Notice that the tolerance of MMI region length is larger than tolerance of width. Therefore, etching the width of the device should ensure high accuracy for the device to operate with the best performance.

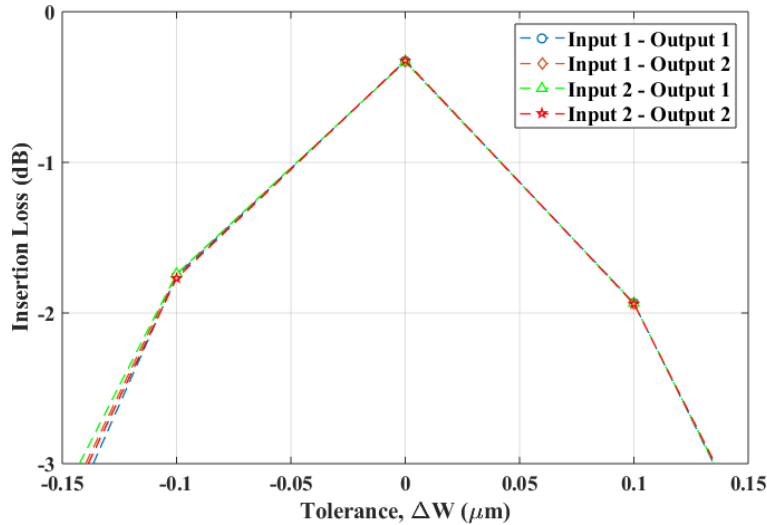


Fig. 7. Tolerance of the proposed switching device on variation of the MMI width

### 3 Evaluation on system

After evaluating the optical conversion efficiency of the device at the physical level, we continue to evaluate this proposed device at the system level. Note that the simulation parameters of optical mode switch in this system are exactly the same as the structure's parameters described above. The switching system is presented in Figure 8. It includes three parts: transmitter, transmission channel and receiver. In the transmitter consists of bit sequence generator, NRZ-pulse generator, laser and Mach-Zehnder modulator. The transmission channel is the switch device. The receiver consists of APD photodiode and BER analyzer.

First, the electric bit strings are generated by the bit sequence generators. These bit strings will be encoded by NRZ encoder before being inserted to the Mach-Zehnder modulator. Next, the Mach-Zehnder modulator combines with laser to produce the light bit strings and launching into the device. After that, the optical signal at the outputs of the device will be taken to the APD photodiode with the aim of converting the optical signal to the electric signal. Finally, BER analyzers will evaluate the system quality through the bit error rate parameter.

We proceed to investigate BER by parameters: wavelength, transmit power and data bit rate.

In the figure 9, two fixed parameters are the bit rate of 30Gbps and the transmitter power of 0dBm. We scan the wavelength from 1.5 $\mu$ m to 1.6 $\mu$ m, the bit error rate is always less than 10<sup>-9</sup>. This bit error rate is also standard when manufacturing device.

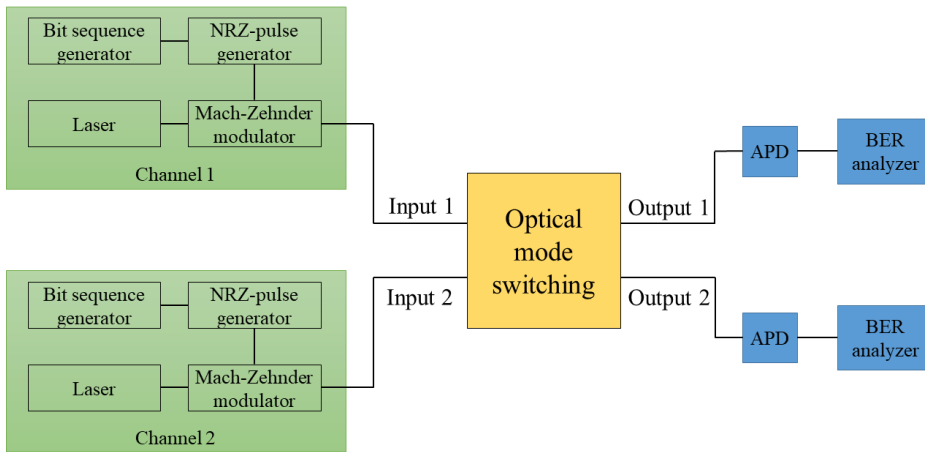


Fig. 8. Switching system model

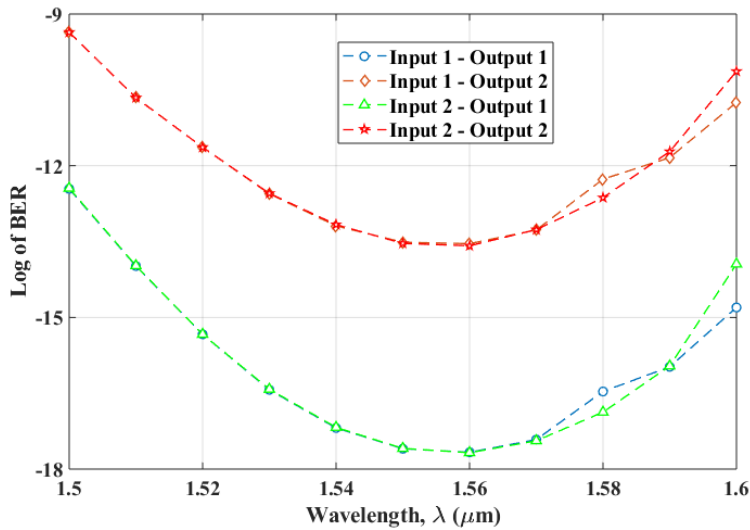


Fig. 9. Bit error rate of the system on variation of the wavelength



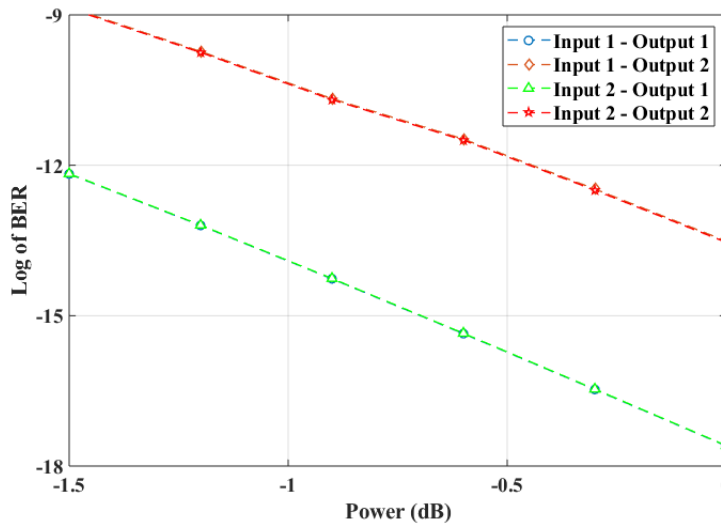


Fig. 10. Bit error rate of the system on variation of the transmitting power

Similarly, figure 10 shows the bit error rate as function of transmitter power with the wavelength and the bit rate are fixed of 1.55 $\mu$ m and 30Gbps, respectively. To achieve the minimum bit error rate of  $10^{-9}$ , the transmitter power must be greater than -1.4dBm.

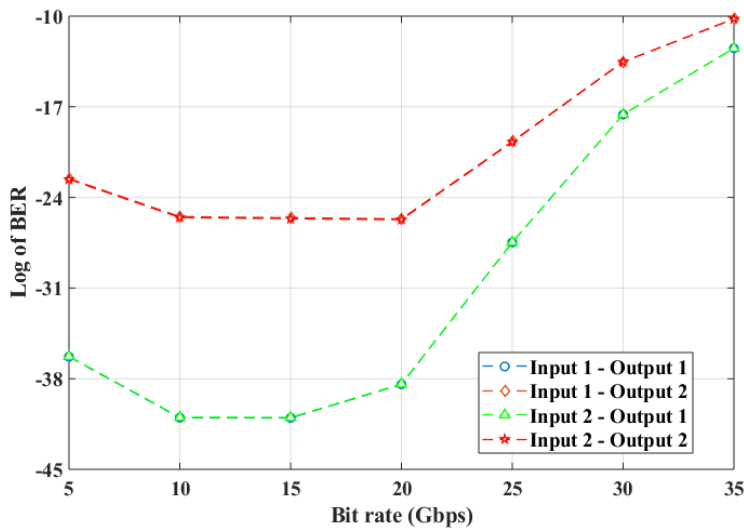


Fig. 11. Bit error rate of the system on variation of the bit rate

Finally, we evaluate quality of the system at the central wavelength of 1.55 $\mu$ m and the transmitter power of 0dBm. From figure 11, the system can operate well bit rate up to 35Gbps with log of BER below -10. The result also shows that the BER ratio gradually decreases as the bit rate increases.

## 4 Conclusion

We have presented a design of an optical mode switching device with the compact size based on SOI material. The device is constructed by two MMIs and a phase shifter which is capable of flexible switching fundamental optical modes from input ports to output ports by changing the phase shifter. This switching device can route TE<sub>0</sub> modes to the arbitrary desired output with a small insertion loss and crosstalk. With these advantages are compact size and large efficiency, we hope that the proposed optical chip is expected to replace electrical chips in the future.

## Reference

1. L. Bassi, "Industry 4.0: Hope, hype or revolution?," RTSI 2017 - IEEE 3rd International Forum on Research and Technologies for Society and Industry, Conference Proceedings. 2017.
2. A. Liu et al., "Wavelength division multiplexing based photonic integrated circuits on silicon-on-insulator platform," *IEEE J. Sel. Top. Quantum Electron.*, vol. 16, no. 1, pp. 23–32, 2010.
3. R. Ryf et al., "Mode-division multiplexing over 96 km of few-mode fiber using coherent 6×6 MIMO processing," *Journal of Lightwave Technology*, vol. 30, no. 4, pp. 521–531, Feb. 2012.
4. N. Hanzawa et al., "Mode-division multiplexed transmission with fiber mode couplers," presented at the Opt. Fiber Commun. Conf./Nat. Fiber Engineers Conf., OSA, Los Angeles, CA, USA, Mar. 4–8, 2012.
5. S. G. Leon-Saval et al., "Mode-selective photonic lanterns for space division multiplexing," *Opt. Exp.*, vol. 22, no. 1, pp. 1036–1044, 2014.
6. T. Mizuno, H. Takara, A. Sano, and Y. Miyamoto, "Dense Space Division Multiplexed Transmission Systems Using Multi-Core and Multi-Mode Fiber," *Journal of Lightwave Technology*, vol. 34, no. 2, pp. 582–592, 2016.
7. Y. Cao, C. Gan, Y. Zhou, L. Shi, and L. Zhu, "A novel architecture of reconfigurable WDM/TDM-PON," WOCC2010 Technical Program - The 19th Annual Wireless and Optical Communications Conference: Converging Communications Around the Pacific, 2010.
8. X. Li, Q. Liu, and R. Hou, "The application of workflow technology on dynamic PDM document management," *Proceedings - 2012 International Conference on Computer Science and Electronics Engineering, ICCSEE 2012*, vol. 2, pp. 559–562, 2012.
9. K. I. Kitayama, N. P. Diamantopoulos, Y. Yoshida, and A. Maruta, "Mode division multiplexed networks," 2017 Opto-Electronics and Communications Conference, OECC 2017 and Photonics Global Conference, PGC 2017, vol. 2017-Novem. pp. 1–3, 2017.
10. Lucas B. Soldano and Erik C. M. Pennings, "Optical Multi-Mode Interference Devices Based on Self-Imaging: Principles and Applications," *Journal of Lightwave Technology*, vol. 13, no. 4, pp. 615–627, 1995.
11. L.-W. Luo, et al., "WDM-compatible mode-division multiplexing on a silicon chip," *Nat. Commun.* 5, pp. 1–7, 2014.
12. T. Uematsu, Y. Ishizaka, Y. Kawaguchi, K. Saitoh, M. Koshihara, Design of a compact two-mode multi/demultiplexer consisting of multimode interference waveguides and a wavelength-insensitive phase shifter for mode division multiplexing transmission, *J. Light. Technol.* 30, pp. 2421–2426, 2012.
13. Y. Liu, J. Yan, G. Han, "The transmission characteristic of metal-dielectric metal slot waveguide-base nanodisk cavity with gain medium," *IEEE Photonics.* 7, pp. 1–8, 2015.

14. Y. Li, C. Li, C. Li, B. Cheng, C. Xue, "Compact two-mode (de)multiplexer based on symmetric y-junction and multimode interference waveguides," *Opt. Express* 22, pp. 5781–5786, 2014.
15. D. Dang, B. Patra, R. Mahapatra, and M. Fiers, "Mode-Division-Multiplexed Photonic Router for High Performance Network-on-Chip," *Proceedings of the IEEE International Conference on VLSI Design*, vol. 2015-Febru, no. February. pp. 111–116, 2015.
16. H. K. T. Xinru Wu, Chaoran Huang, Ke Xu, Chester Shu, "Mode-Division Multiplexing for Silicon Photonic Network-on-Chip.," *Journal of Lightwave Technology*, pp. 3223–3228, 2017.
17. Y. Xiong, R. B. Priti, and O. Liboiron-Ladouceur, "High-speed two-mode switch for mode-division multiplexing optical networks," *Optica*, vol. 4, no. 9, p. 1098, 2017.
18. Q. Lai, W. Hunziker, and H. Melchior, "Low-power compact  $2 \times 2$  thermo-optic silica-on-silicon waveguide switch with fast response," *IEEE Photonics Technology Letters*, vol. 10, no. 5. pp. 681–683, 1998.
19. L. B. Soldano, E. C.M. Pennings, "Optical multi-mode interference devices based on self-imaging: Principles and applications," *Journal of Lightwave Technology*, 13, pp. 615–627, 1995.